Simplified Control for Redistributive Balancing Systems using Bidirectional Flyback Converters

Lucas McCurlie, Matthias Preindl, Pawel Malysz, Ali Emadi
Department of Electrical and Computer Engineering, McMaster University
Hamilton, Ontario, Canada L8S 4L7
E-mail: mccurllb@mcmaster.ca, preindl@mcmaster.ca

***Abstract*—Battery stacks with many cells per string require sophisticated balancing hardware for capacity maximization, safe operation, and extended lifetime. This paper proposes a simplified control architecture for redistributive battery balancing topologies. A high level controller defines the link currents to be actuated by flyback DC/DC converters. Linear transformations are used to rewrite the balancing problem as a regulation problem that can be solved with a saturated LQR. To reduce the overall system complexity and cost, the low-level control requirements are minimized using feedforward approaches based on pulse width and pulse frequency modulation. The control system is developed using MATLAB/Simulink/PLECS and validated experimentally.**

I. Introduction

Lithium Ion batteries are widely used in many applications because of their high energy density, low self-discharge rate and high cell voltage. Batteries are connected in series in order to achieve higher voltages but this can lead to exponential reduction of the battery life as the number of cells increases [1]. Cell imbalances arise due to internal effects such as manufacturing inconsistencies, different self-discharge rates and internal resistance as well as external effects such as temperature variations. To avoid damages, correct any imbalances and improve the effective capacity of the pack, an energy balancing system is required.

A balancing system can be divided into two main classes; dissipative and non-dissipative. A dissipative approach draws excess charge from cells with higher state of charge and dissipates it through resistors. A non-dissipative approach uses power electronics to transfer charge between cells. Redistributive techniques and various hardware topologies have been studied and applied in industry [2] [3] [4]. The two main redistributive methods are cell to cell (C2C) which transfers charge between adjoining cells, cell to stack (C2S) which transfers charge from one cell to the entire stack and stack to cell (S2C) which is the opposite case of C2S by transferring the charge from the entire stack to just one cell.

Both classifications can further be divided into passive balancing and active balancing. Passive balancing relies on system properties and does not require a controller. Faster balancing can be achieved using active balancing systems which use a high level controller to direct the charge and discharge currents per cell.

In our study, we will examine redistributive active balancing systems on the example of C2S and S2C using flyback DC/DC converters to realize the battery links. We propose a simplified control system that has a structure similar to [5]. First the balancing problem is transformed into a regulation problem. This problem is solved with a saturated (LQR) controller. This controller defines currents in links that have to be applied by DC/DC converters. DC/DC converters have their own control structure. To reduce the per link complexity, feedforward current controllers are proposed. Possible offsets are removed by the high level controller. This is validated using MATLAB/Simulink/PLECS as well as experimentally. The nomenclature used in this paper is shown in TABLE I.

II. System Description

A. Battery System

A redistributive balancing system based on a cell to stack approach can be seen in Fig. 1. The battery cells within the stack can be described by the amount of charged stored $\mathbf{Q}_x x(t)$. The vector $x(t) \in [0,1]^n$ is the state of charge (0 corresponds to an empty cell and 1 corresponds to a full cell). $\mathbf{Q}_x \in \mathbb{R}^{n\times n}$ defines charge capacities along a diagonal matrix as follows

$$\mathbf{Q}_x = \begin{bmatrix} q_1 & 0 & \dots & 0 \\ 0 & q_2 & \dots & 0 \\ 0 & 0 & \dots & 0 \\ 0 & 0 & \dots & q_n \end{bmatrix},$$

where $q_1 ... q_n$ are the capacities of cell 1 to n respectively. The balancing currents which control the state of charge is $\mathbf{Q}_u u(t)$ where $u(t) \in [-1,1]^m$ is the normalized balancing currents

TABLE I
Balancing System Parameters

Variable	Value/Unit
Cell side inductance L_c	3.05 μH
Stack side inductance L_s	$N^2 L_c$ μH
Switching Frequency F_s	70 - 105 KHz
Turns Ratio N	2
Number of cells n	4
Cell voltage V_{cj}	2.5 to 4.2 V
Stack voltage V_s	$\sum_{j=1}^{n}(V_{cj})$ V
Instantaneous Primary current i_{pj}	A
Instantaneous Secondary current i_{sj}	A
Primary peak current i_{pkp}	A
Secondary peak current i_{pks}	A
Average cell current i_{c_j}	A

978-1-4673-6741-7/15/$31.00 ©2015 IEEE

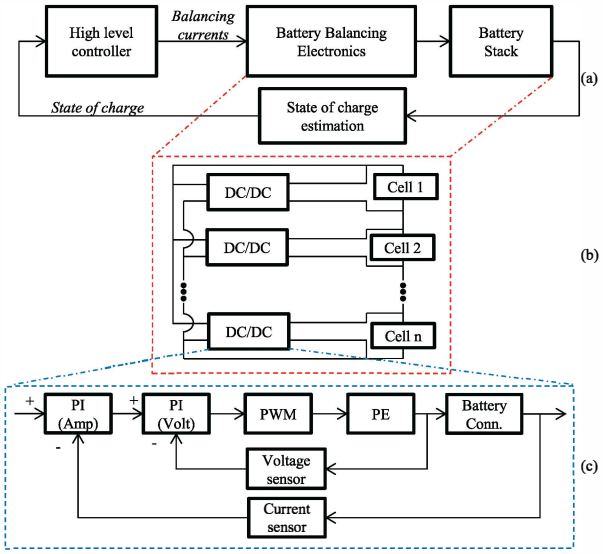

Fig. 1. Balancing system (a); based on the bidirectional (C2S/S2C) topology used as an example (b); typical low level control of a single PE module (c).

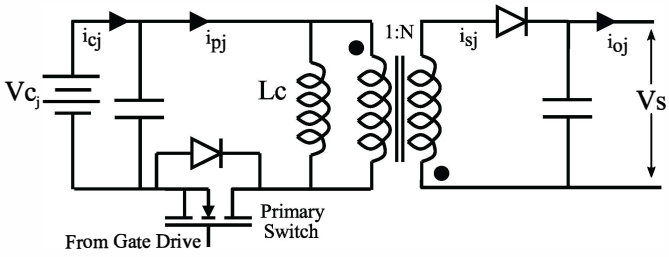

Fig. 2. Uni-directional flyback converter.

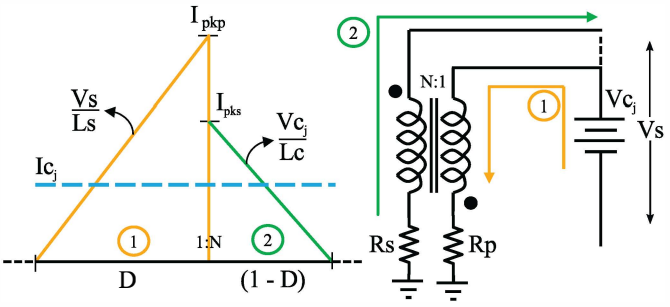

Fig. 3. Discharging (C2S) waveform with Hardware relationship; orange lines are instantaneous primary current i_{p_j}; green lines indicate instantaneous sec. current i_{s_j}; thick blue lines are cell average currents i_{c_j}.

and $\mathbf{Q}_u \in \mathbb{R}^{m\times m}$ defines current capacities of each link [4] as follows

$$\mathbf{Q}_u = \begin{bmatrix} I_{max_1} & 0 & \dots & 0 \\ 0 & I_{max_2} & \dots & 0 \\ 0 & 0 & \dots & 0 \\ 0 & 0 & \dots & I_{max_m} \end{bmatrix},$$

where $I_{max_1}...I_{max_m}$ are the maximum currents for link 1 to m respectively. The state of charge of the system can be modeled by

$$x^+ = x + \mathbf{B}u, \tag{1}$$

where $\mathbf{B} = \mathbf{Q}_x^{-1}\mathbf{T}\mathbf{Q}_u$. The topology matrix $\mathbf{T}$ defines how the balancing charge is transferred via the links [4]. This paper uses the cell to stack topology, which is defined by

$$\mathbf{T} = \begin{bmatrix} \frac{1}{n}-1 & \frac{1}{n} & \dots & \frac{1}{n} \\ \frac{1}{n} & \frac{1}{n}-1 & \dots & \frac{1}{n} \\ \frac{1}{n} & \frac{1}{n} & \dots & \frac{1}{n} \\ \frac{1}{n} & \frac{1}{n} & \dots & \frac{1}{n}-1 \end{bmatrix} \in \mathbb{R}^{m\times n}.$$

The balancing currents are limited by the maximum current that can be transferred by a link. The inputs u are subject to polyhedral constraints that dependent on the topology [4] [5]. These constraints are written as the equality constraint $\mathbf{H}_{eq}u = K_{eq}$ and the inequality constraint $\mathbf{H}_u u \leq K_u$.

B. High level control

The top level controller balances the cells actuating currents in the links. This requires information regarding the state of charge of each battery cell. The state of charge x is not measurable but can be estimated according to $y = C(x)$ where y is the voltage associated with the terminals of the battery and C is a nonlinear mapping [6]. Simple estimation techniques are voltage lookup tables and coulomb counting [7] [8]. More sophisticated SOC estimation techniques are Kalman filters [9], neural networks [10] and fuzzy logic [11]. In this work, we assume the SOC is reconstructed with sufficient precision.

Balancing control can be implemented with different strategies such as rule based approaches [12], optimization algorithms [4] [13] and fuzzy logic [14]. In designing the LQR, we first need to transform (1) into a regulation problem using $\bar{x} = \mathbf{L}x$ where $\mathbf{L}$ is defined in [4] and the balanced state is when $\bar{x} = 0$. The equality constraint is removed using the transformation

$$u = \mathbf{F}\bar{u} + u_0, \tag{2}$$

where $\mathbf{F}$ is the nullspace of $\mathbf{H}_{eq}$, such that $\mathbf{F}\mathbf{H}_{eq} \equiv 0$ and u_0 is any solution of $\mathbf{H}_{eq}u_0 = \mathbf{K}_{eq}$. This will yield the system

$$\bar{x}^+ = \bar{x} + \bar{\mathbf{B}}\bar{u} + \mathbf{L}\mathbf{B}u_0, \tag{3}$$

where $\bar{\mathbf{B}} = \mathbf{L}\mathbf{B}\mathbf{F}$. The component $\mathbf{L}\mathbf{B}u_0$ is a non-zero offset value in general that can be removed by integration. However, $\mathbf{L}\mathbf{B}u_0 \equiv 0$ for all topologies studied in [4]. The updated system (3) is linear, thus we can define a discrete, infinite-time Linear Quadratic Regulator (LQR) that minimizes the cost function $J = \sum_{k=0}^{\infty}(\bar{x}_k^T\mathbf{Q}\bar{x}_k + \bar{u}_k^T\mathbf{R}\bar{u}_k)$.

The LQR problem is solved by a regular feedback controller defined as

$$\bar{u}_k = -\mathbf{F}_{lqr}\bar{x}_k, \tag{4}$$

where $\mathbf{F}_{lqr}$ is found by solving the discrete time Riccati equation. However, the controller input may not satisfy the inequality constraints. Thus, the input is saturated such that it satisfies the inequality constrains according to

$$\bar{\mathbf{H}}\bar{u} \leq \bar{K}, \tag{5}$$

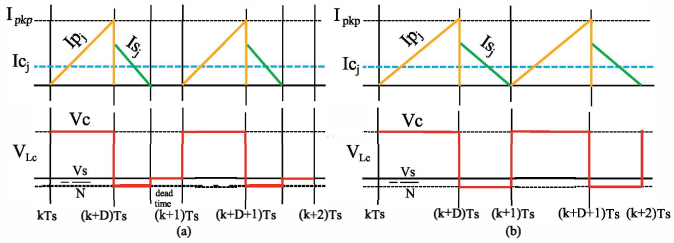

Fig. 4. Ideal PWM cell/stack waveforms (a) above; voltage across inductor V_{Lc} (a) below; ideal PFM cell/stack waveforms (b) above; voltage across inductor V_{Lc} (b) below.

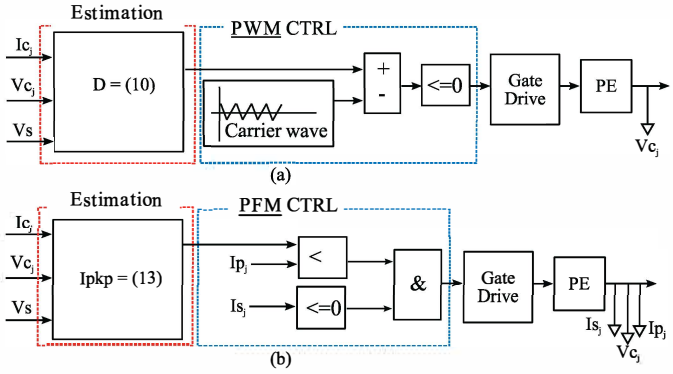

Fig. 5. Estimation and control implementation; PWM (a); PFM (b).

where $\bar{\mathbf{H}} = \mathbf{HF}$ and $\bar{K} = K - \mathbf{H}u_0$. The result is transformed into a control input for the original system with (2). The saturation (5) ensures that the inequality constraints are satisfied and the transformation (2) ensures that the equality constraints are met. Hence, the resulting back-transformed u is feasible. Also, the resulting closed loop system is stable according to [15] [16]. This input u defines the average balancing currents in each link according to

$$\mathbf{Q}_u u(t) = [i_{c_1}, i_{c_2}, i_{c_3} ... i_{c_m}]. \tag{6}$$

C. Redistributive Power Electronics: analysis of a flyback converter

Fig. 1(b) shows the balancing hardware and the stack of cells. The combined stack voltage V_s is much greater than the individual cell voltage V_c in automotive battery packs. The redistributive hardware requires links that connect cells at different potentials. Isolated DC/DC converters are typically used to keep the power rating of the switches low [4]. A simple implementation can be done using flyback converters, which are used since the power level is relatively low. We analyze the converter in a unidirectional state depicted in Fig. 2. The converter is operated in Discontinuous Conduction Mode (DCM) because it requires a smaller transformer, reducing system costs than its Continuous Conduction Mode (CCM) counterpart [17]. The behavior of the isolated transformer can be modeled by an ideal transformer in parallel with a magnetizing inductance. Derived from the buck-boost converter, when the primary switch is closed Fig. 2, the diode is reverse biased due to the winding polarities and the inductor voltage $V_{Lc} = V_c$. The current through the cell during the on-time of the primary switch is

$$L_c \frac{di_p(t)}{dt} = V_{Lc} \Rightarrow \frac{i_{pkp}}{DT_s} = \frac{V_c}{L_c}. \tag{7}$$

The transformer (main inductance) stores energy during the on-time. When the primary switch is opened, this energy is transferred to the secondary winding, forward biasing the diode and supplying the load. In this state, the instantaneous cell current becomes zero, $i_{p_j} = 0$ and the inductor voltage becomes $V_{Lc} = -\frac{V_s}{N}$. The average link current is then defined as

$$i_{c_j} = \frac{1}{T_s} \int_0^{T_s} i_{p_j} dt = \frac{i_{pkp} D}{2}, \tag{8}$$

where D is the duty cycle of the pulse width modulation (PWM). The voltage and current waveforms for the flyback circuit operating with PWM are shown in Fig. 4(a).

III. Low Level Control

The high level controller (6) defines an average balancing current i_{c_j} for each DC/DC converter. The low level controller actuates this average link current. A typical control architecture is shown in Fig. 1(c) which regulates the output voltage based on an outer feedback current control loop using PWM. The PI controller will determine an appropriate duty ratio which corresponds to the i_{c_j} from the balancing controller. As an example, this low level control is a common implementation for a power supply. However, for battery balancing applications, hundreds of cells in series have a significant impact on the overall system complexity and cost.

By understanding some basic details regarding the internal power electronics, which in this case is the flyback converter, different estimation schemes can be developed such as Pulse Width Modulation (PWM), Pulse Frequency Modulation (PFM) and Constant Operating Point Modulation (COPM). The estimation strategy can be used to simplify the system instead of using the feedback controller in Fig. 1(c). The high level controller will eliminate any steady state errors and the overall complexity of the system can be reduced. Further details on these strategies can be found in [18].

A. Pulse Width Modulation (PWM)

PWM transforms a duty cycle into a switching (gate signal) sequence with a fixed switching frequency. The switching signal is produced by subtracting an input signal with the carrier wave and checking if it is below zero. This is shown in Fig. 5(a). PWM converters can provide predictable operating frequencies which can result in simplifying the design of the circuitry as well as offer low output ripple characteristics and high efficiency during moderate to high load conditions [18].

By estimating the duty cycle of the PWM converter, an estimation strategy can be developed to reduce system cost of extra sensors and analog to digital converters. The charge transferred by each cell for each cycle of the flyback converter

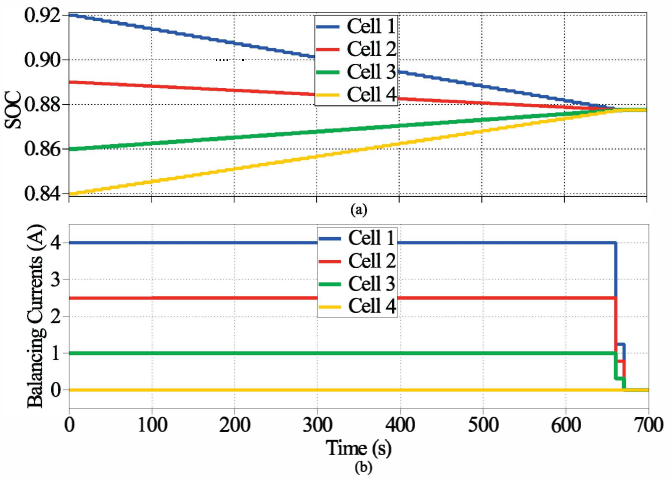

Fig. 6. High level balancing of 4 cells; converging state of charge values (a); applied balancing currents i_{c_j} (b).

is defined as

$$Q_c = \frac{1}{2} i_{pkp} D T_s. \tag{9}$$

By combining (7) and (8) we obtain an equation which describes the average link current I_{c_j} and by re-arranging this equation, a duty ratio can be used with PWM as a feedforward actuation method shown by Fig. 5(a)

$$i_{c_j} = \frac{D^2 T_s V_c}{2L_c} \Rightarrow D = \sqrt{\frac{2 i_{c_j} L_c}{V_c T_s}}. \tag{10}$$

B. Pulse Frequency Modulation (PFM)

Using PWM is a design choice and requires the generation of a carrier wave (internal counter). Pulse frequency modulation is an alternative method used in industry which uses a variable switching frequency. The basic principle of PFM can be understand by the block diagram contained inside the blue dotted line in Fig. 5(b). When the instantaneous primary current hits a peak value, the primary switch turns off until the instantaneous secondary current is driven to zero. This method acts similar to a comparator or a hysteresis based strategy. The main drawback to this method is that it yields variable switching frequencies which make it difficult to predict losses in the semi-conductors [18].

By using a model based predicted peak current I_{pkp} with PFM, we can obtain an estimated average link current I_{c_j}. An estimation strategy can be developed by defining the stack side's current equation during the off-time of the primary switch as follows

$$L_s \frac{di_s(t)}{dt} = V_{Ls} \Rightarrow \frac{i_{pks}}{(1-D)T_s} = \frac{V_s}{L_s}. \tag{11}$$

By combining (7) and (11), D and T_s can be obtained as

$$D = \frac{V_s}{V_s + NV_c}, \; T_s = \frac{i_{pks} L_c}{D V_c}. \tag{12}$$

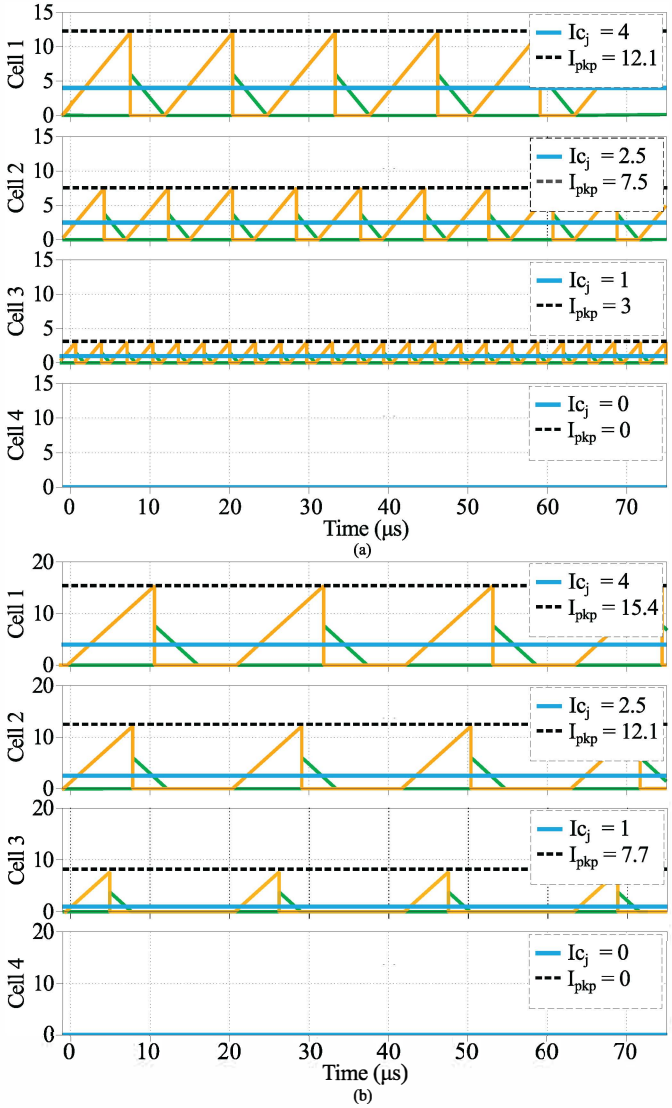

Fig. 7. Simulated results; PFM (a); PWM (b); orange lines indicate instantaneous primary current i_{p_j}; green lines indicate instantaneous sec. current i_{s_j}.

Now from (8) and (12) we can define the predicted average link current through the converter during any given T_s period as well as re-arrange it for a peak limit of the instantaneous current as shown by Fig. 3

$$i_{c_j} = \frac{V_s i_{pkp}}{2(V_s + NV_c)} \Rightarrow i_{pkp} = \frac{2 i_{c_j} (V_s + NV_c)}{V_s}. \tag{13}$$

C. Constant Operation Point Modulation (COPM)

A third strategy emerges by combining the previous two. The actuation can be applied by keeping a constant operating point in low level control. The resulting DC/DC converter is either "on" transferring a given current or "off". This type of operation is suitable for battery balancing but requires a "high level PWM". This high level actuator applies an average current by keeping the DC/DC converter "on" for a larger sampling time and turns it off for the rest. COPM is easily

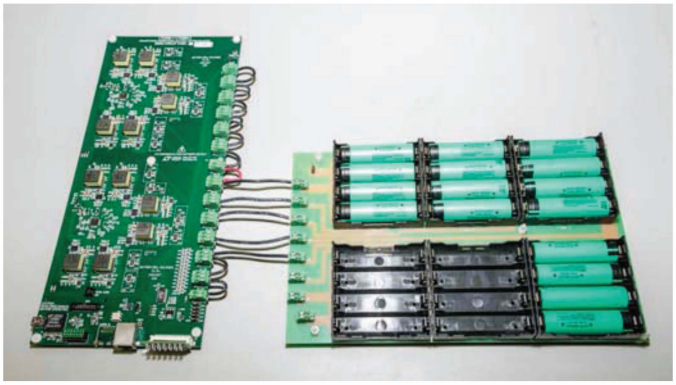

Fig. 8. Experimental test bench; batteries (Panasonic NCR 18650); balancing hardware (Linear Technology DC2100A).

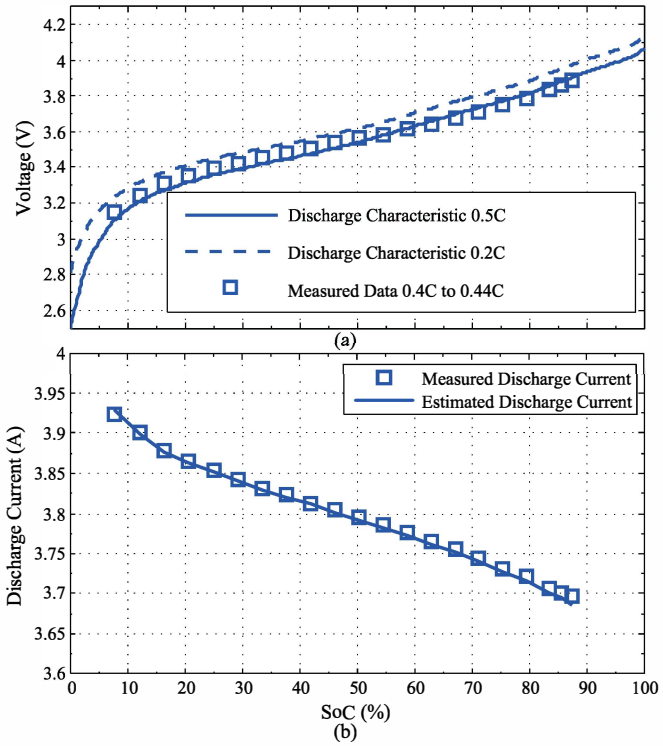

Fig. 9. Measured results (Cell 1 discharge sweep); voltage vs. SOC (a); average link current i_{c_j} Measured Vs. Estimated (b).

accessible because integrated chips for controlling multiple flyback converters are available. An example of such chips is the LTC 3300 from Linear Technology.

IV. Simulated Results

In this section, PWM, PFM and COPM control structures are evaluated. The system parameters are shown in TABLE I. A simulated model of the battery, the power electronics (DC/DC bidirectional flyback converters) and the controller were all designed and tested using Matlab Simulink with the addition of PLECs blocks. Using the high level LQR control implementation from section II-B, the high level balancing currents (6) are defined by Fig. 6(b). The high level controller

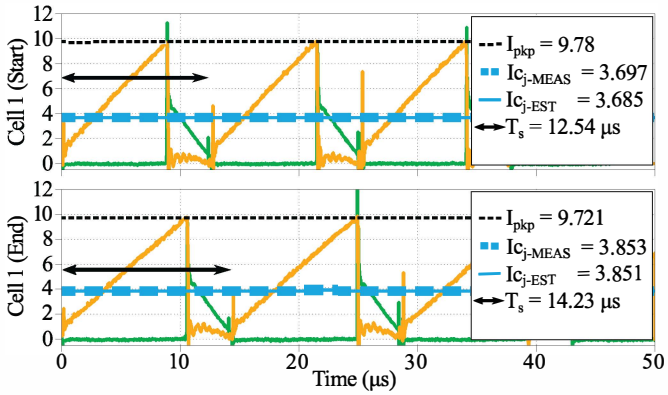

Fig. 10. Measured discharge waveforms; orange lines indicate instantaneous primary current i_{p_j}; green lines indicate instantaneous sec. current i_{s_j}.

balances the state of charge values in Fig. 6(a).

The low level control results for PFM and PWM can be shown by Fig. 7(a) and Fig. 7(b) respectively. These results had identical converging state of charge values shown by Fig. 6(a). This demonstrates that the low level control implementation can be reduced from a typical feedback current control loop to a feedforward actuator of average current using model based estimation. This method has been combined with PWM, PFM and COPM type strategies yielding good results.

V. Experimental Results

The results obtained in this section are tested using the experimental bench in Fig. 8. This test bench is comprised of a LTC DC2100A Demo board and a custom built battery pack using Panasonic NCR 18650 cells. In order to handle the high current transfer that the bidirectional redistributed hardware produces, four Lithium ion cells are placed in parallel making a module. Then four modules are placed in series making the pack. Due to its simplicity, the feedforward actuation described in section III-C has been implemented.

As a proof of concept test, a constant discharge test was conducted on the first cell in the stack as shown by Fig. 9. Using an oscilloscope, the low level instantaneous currents were measured and can be shown by Fig. 10. At the beginning of discharge, the measured current is 3.697A which was obtained using a ammeter in the direct path of the first link. The estimated current for that link was 3.685A. At the end of discharge, the measured current is 3.851A. The estimated current for that link was 3.853A.

The LQR controller described in section II-B was implemented on the test bench. The high level controller balances the state of charge values in Fig. 11(a). The balancing currents defined by Fig. 11(b) are actuated by the low level control strategy described in section III-C. These results demonstrate that a LQR controller is capable of balancing the state of charge of the cells inside a battery pack. We simplify the low level control by replacing the feedback current control loop with a feedforward average current actuation strategy. Possible actuation errors are compensated by the LQR. This

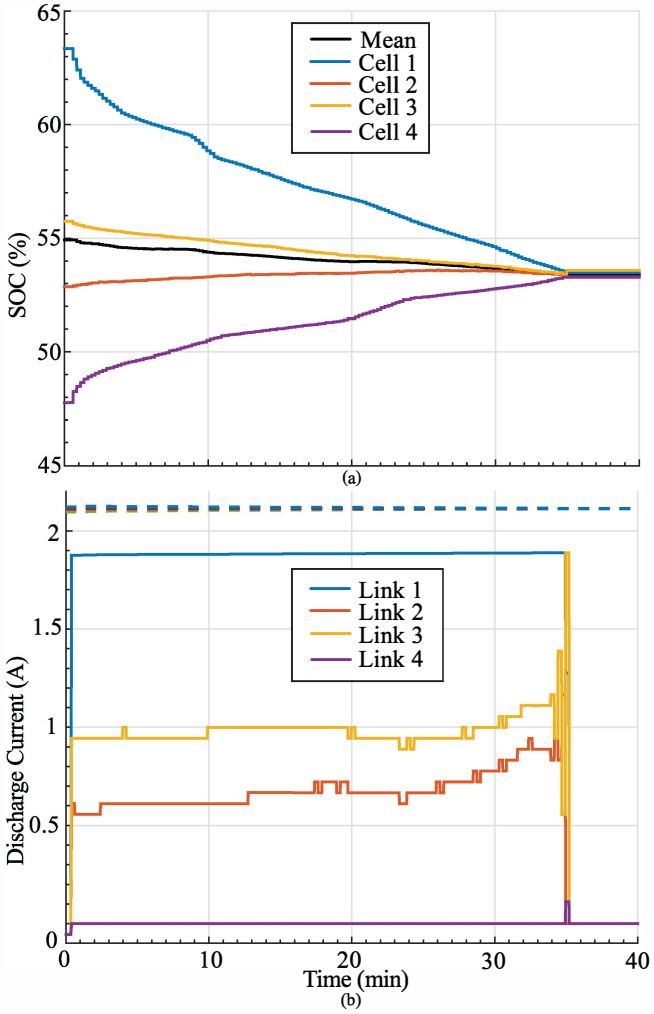

Fig. 11. LQR measured results; balancing state of charge $x(t)$ (a); applied balancing current $\mathbf{Q}_u u(t)$ (b).

is confirmed since it is shown that the SOCs of each cell converge to the average SOC of the pack.

VI. Conclusions

This paper proposes a simplified control approach for non-dissipative balancing of battery packs comprising of battery cells, balancing links, and a control system. A high level LQR is designed to balance, i.e. equalize, the state-of-charge (SoC) of the battery cells. Linear transformations are used to transform the control into a regulation problem and to ensure that the control input is feasible. The high level controller is based on a general battery pack model that can be adopted for cells with different capacities since each cell is modeled by its capacity and state-of-charge. Also, it can be combined with various battery balancing topologies that are modeled by a topology matrix and the maximum current in each link.

In practice, balancing links are (isolated) DC/DC converters that actuate the (average) balancing current defined by the high level controller. Traditionally, this requires a low-level current control loop. This paper proposes to simplify the setup (sensors, ADC, etc.) using a model-based feedforward actuation scheme. This scheme has been combined and tested in simulation with different modulation schemes: pulse width modulation (PWM), pulse frequency modulation (PFM), and Constant Operating Point Modulation (COPM). The proposed control system with LQR and COPM-based feedforward actuation was implemented and validated on an experimental test bench that consists of a battery module and the cell-to-stack battery balancing topology.

VII. Acknowledgements

This research was undertaken, in part, thanks to funding from the Canada Excellence Research Chairs Program.

References

[1] N. Kutkut, H. Wiegman, D. Divan, and D. Novotny, "Charge equalization for an electric vehicle battery system," *Aerospace and Electronic Systems, IEEE Transactions on*, vol. 34, no. 1, pp. 235–246, Jan 1998.

[2] N. Kutkut and D. Divan, "Dynamic equalization techniques for series battery stacks," in *Telecommunications Energy Conference, 1996. INTELEC '96., 18th International*, Oct 1996, pp. 514–521.

[3] J. Cao, N. Schofield, and A. Emadi, "Battery balancing methods: A comprehensive review," in *Vehicle Power and Propulsion Conference, 2008. VPPC '08. IEEE*, Sept 2008, pp. 1–6.

[4] M. Preindl, C. Danielson, and F. Borrelli, "Performance evaluation of battery balancing hardware," in *Control Conference (ECC), 2013 European*, July 2013, pp. 4065–4070.

[5] M. Caspar and S. Hohmann, "Optimal cell balancing with model-based cascade control by duty cycle adaption," *19th IFAC World Congress*, vol. 1, pp. 1–1, 2014.

[6] B. Xiao, Y. Shi, and L. He, "A universal state-of-charge algorithm for batteries," in *Design Automation Conference (DAC), 2010 47th ACM/IEEE*, June 2010, pp. 687–692.

[7] K.-S. Ng, Y.-F. Huang, C.-S. Moo, and Y.-C. Hsieh, "An enhanced coulomb counting method for estimating state-of-charge and state-of-health of lead-acid batteries," in *Telecommunications Energy Conference, 2009. INTELEC 2009. 31st International*, Oct 2009, pp. 1–5.

[8] A. Ausswamaykin and B. Plangklang, "Design of real time management unit for power battery in pv-hybrid power supplies by application of coulomb counting method," in *Electrical Engineering Congress (iEECON), 2014 International*, March 2014, pp. 1–4.

[9] G. L. Plett, "Extended kalman filtering for battery management systems of lipb-based {HEV} battery packs: Part 1. background," *Journal of Power Sources*, vol. 134, no. 2, pp. 252 – 261, 2004.

[10] M. Charkhgard and M. Farrokhi, "State-of-charge estimation for lithium-ion batteries using neural networks and ekf," *Industrial Electronics, IEEE Transactions on*, vol. 57, no. 12, pp. 4178–4187, Dec 2010.

[11] R. Feng, S. Zhao, and X. Lu, "On-line estimation of dynamic state-of-charge for lead acid battery based on fuzzy logic," in *Measurement, Information and Control (ICMIC), 2013 International Conference on*, vol. 01, Aug 2013, pp. 447–451.

[12] M. Daowd, M. Antoine, N. Omar, P. Lataire, P. Van Den Bossche, and J. Van Mierlo, "Battery management systembalancing modularization based on a single switched capacitor and bi-directional dc/dc converter with the auxiliary battery," *Energies*, vol. 7, no. 5, pp. 2897–2937, 2014.

[13] F. Baronti, R. Roncella, and R. Saletti, "Performance comparison of active balancing techniques for lithium-ion batteries," *Journal of Power Sources*, vol. 267, no. 0, pp. 603 – 609, 2014.

[14] J. Yan, Z. Cheng, G. Xu, H. Qian, and Y. Xu, "Fuzzy control for battery equalization based on state of charge," in *Vehicular Technology Conference Fall (VTC 2010-Fall), 2010 IEEE 72nd*, Sept 2010, pp. 1–7.

[15] E. D. Sontag, "An algebraic approach to bounded controllability of linear systems," *Int. J. Control*, vol. 39, pp. 181–188, 1984.

[16] J. Choi, "On the stabilization of linear discrete time systems subject to input saturation," *Systems and Control Letters*, vol. 36, no. 3, pp. 241 – 244, 1999.

[17] A. A. Saliva, "Design guide for off-line fixed frequency dcm flyback converter," Infineon, Tech. Rep., 2013, design note DN 2013-01.

[18] U. Sengupta, "Pwm and pfm operation of dc/dc converters for portable applications," in *TI Portable Power Design Seminar*, 2006.